Virus Research 270 (2019) 197670

Contents lists available at ScienceDirect

Virus Research

journal homepage: www.elsevier.com/locate/virusres

# Identification of a functional nuclear localization signal in 3D$^{pol}$/3CD of duck hepatitis A virus 1

Jun-Hao Chen[a,b], Rui-Hua Zhang[a,b], Shao-Li Lin[a,b], Peng-Fei Li[a,b], Jing-Jing Lan[a,b], Ji-Ming Gao[c], Zhi-Jing Xie[a,b], Fu-Chang Li[d], Shi-Jin Jiang[a,b,*]

[a] College of Veterinary Medicine, Shandong Agricultural University, Shandong Taian, 271018, China
[b] Shandong Provincial Key Laboratory of Animal Biotechnology and Disease Control and Prevention, Taian, 271018, China
[c] Department of Basic Medical Sciences, Taishan Medical College, Taian, 271000, China
[d] College of Animal Science and Technology, Shandong Agricultural University, Taian, 271018, China

ARTICLE INFO

*Keywords:*
DHAV-1
3D$^{pol}$
3CD
NLS

ABSTRACT

The nuclear localization signals (NLS) were usually composed of basic residues (K and R) and played an important role in delivery of genomes and structural protein into nucleus. In this research, we identified that 3D$^{pol}$/3CD entered into nucleus during viral propagation of duck hepatitis A virus type 1 (DHAV-1). To investigate the reason that 3D$^{pol}$/3CD entered into nucleus, the amino acid sequence of 3CD was analyzed through NLS Mapper program. The basic region $^{17}$PRKTAYMRS$^{25}$ was subsequently proved to be a functional NLS to guide 3D$^{pol}$/3CD into nucleus. $^{18}$R, $^{19}$K and $^{24}$R were found essential for maintaining the nuclear targeting activity, and exchange between $^{24}$R and $^{24}$K had no impact on cellular localization of 3D$^{pol}$. Since the entry of 3D$^{pol}$/3CD into nucleus was essential for shutoff of host cell transcription and maintaining the viral propagation of picornavirus numbers, our study provided new insights into the mechanism of DHAV-1 propagation.

## 1. Introduction

Duck viral hepatitis (DVH) is an acute and highly fatal disease of young ducklings that characterized by severe liver bleeding and opisthotonos. DVH was first described in the United States in 1949 (Levine and Fabricant, 1950). In China, DVH emerged in 1963, and the pathogen was formally identified in 1984 (Guo and Pan, 1984). DVH is caused by duck hepatitis virus types 1 (DHV-1), 2 and 3, yet there was no antigenic relationships among them (Haider and Calnek, 1979; Toth, 1969). DHV-1 was classified as a member of *Picornaviridae* and renamed as duck hepatitis A virus (DHAV) according to the Virus Taxonomy ninth Report of the International Committee on Taxonomy of Viruses (ICTV) (Knowles et al., 2012). Based on the phylogenetic analyses and neutralization tests, DHAV was further classified into three serotypes: DHAV-1 (the classical serotype 1) (Gao et al., 2012; Kim et al., 2006), DHAV-2 (a serotype isolated in Taiwan) (Tseng and Tsai, 2007), and DHAV-3 (a serotype isolated in South Korea and China) (Kim et al., 2007; Xu et al., 2012). There was limited cross-neutralization between DHAV-1 and DHAV-3 (Tseng and Tsai, 2007), yet no cross-neutralization was found between DHAV-1 and DHAV-2 (Kim et al., 2007). DHAV-1 is the only member of novel genus *Avihepatovirus* of family *Picornaviridae*. The viral genome of DHAV-1 was a positive, single-stranded, non-enveloped RNA of ˜7700-nucleotide. The genomic RNA contains a 5′ untranslated region (5′ UTR), one open reading frame (ORF) that encodes three structural proteins (VP0, VP1 and VP3) and nine nonstructural proteins (2A1, 2A2, 2A3, 2B, 2C, 3A, 3B, 3C and 3D), and a 3′ UTR plus poly(A) tail (Kim et al., 2006).

In infected host cells, viral gene products crossing the nuclear envelope need the assistance from nuclear transport apparatus to shutoff host cell transcription or start viral transcription (Sharma et al., 2004). The nuclear import of macromolecules is a signal-mediated, energy-dependent and highly selective process (Gorlich and Mattaj, 1996). The small molecules, such as ions, metabolites, and globular protein that smaller than 40 kDa can freely cross the nuclear envelope through numerous pores into nucleus (McLane and Corbett, 2009). Proteins over 40 kDa weight are too large for the pore complex to accumulate in the nucleus unless they own nuclear localization signal (NLS) sequence. The NLS normally located near the C-terminal of the protein (McLane and Corbett, 2009), and guided the protein transportation into nucleus through binding to nuclear import receptors including importin α and β (Goldfarb et al., 2004).

The viral capsid proteins normally distributed in the cytoplasm and functioned in assembling viral particles, which were also found localizing in the nucleus with the assistance of NLS (Colpitts et al., 2011; Pei

* Corresponding author at: College of Veterinary Medicine, Shandong Agricultural University, 61 Daizong Road, Taian, 271018, China.
*E-mail address:* sjjiang@sdau.edu.cn (S.-J. Jiang).

https://doi.org/10.1016/j.virusres.2019.197670
Received 23 January 2019; Received in revised form 16 July 2019; Accepted 17 July 2019
Available online 19 July 2019
0168-1702/ 

et al., 2008; Wang et al., 2012; Wychowski et al., 1985; Xiang et al., 2013). To picornaviruses, the functional protein 3D polypeptides ($3D^{pol}$) plays an important role in viral replication by acting as an RNA-dependent RNA polymerase (RdRP) (Gong and Peersen, 2010; Marcotte et al., 2007; Nguyen et al., 2013; Shatskaya et al., 2013; Sierra et al., 2007; Zhang et al., 2017). The $3D^{pol}$ and viral protease-polymerase precursor 3CD of some picornaviruses were found localizing in the nucleus of infected cells (García-Briones et al., 2006; Sanchez-Aparicio et al., 2013; Sharma et al., 2004). The recent investigation showed that the 2A protease ($2A^{pro}$) was also necessary for 3CD of rhinovirus to cross into the nucleus (Walker et al., 2016).

Up till now, it is still unclear how the viral components of DHAV-1 entered into nucleus to shutoff cellular transcripts and maintain high viral replication efficiency. The DHAV-1 $3D^{pol}$ possessed RdRP activity (Zhang et al., 2017), so it might play important role during RNA genome replication in the cytoplasm. In this research, $3D^{pol}$/3CD of DHAV-1 was found entering into nucleus during DHAV-1 viral propagation. To explore how the $3D^{pol}$/3CD enters into nucleus, the amino acid sequence of 3CD were analyzed through NLS Mapper program (http://nls-mapper.iab.keio.ac.jp/cgi-bin/NLS_Mapper_form.cgi). The results showed that the basic region $^{17}$PRKTAYMRS$^{25}$ was a functional NLS to guide $3D^{pol}$/3CD into nucleus, and $^{18}$R, $^{19}$K and $^{24}$R were essential for maintaining the nuclear targeting activity of $3D^{pol}$.

## 2. Materials and methods

### 2.1. Cells, virus and cell transfection

Baby Hamster Syrian Kidney cells (BHK-21, ATCC® CCL-10™), duck embryo fibroblasts (DEFs, ATCC® CCL-141) or Chinese hamster ovary cells (CHO, ATCC® CRL-12023) were cultured at 37 °C in 5% $CO_2$ in Dulbecco's modified Eagle medium (DMEM; Gibco, Carlsbad, CA, USA) supplemented with 10% fetal bovine serum (FBS; Gibco), 100 units/ml penicillin, and 100 μg/ml Streptomycin Sulfate. LY0801 (accession no. FJ436047) is a virulent strain of DHAV-1 isolated in 2008 from an outbreak of severe DVH in Shandong province, China (Gao et al., 2012). For DNA transfection, 4.0 μg of recombinant plasmids were diluted in 250 μL of opti-MEM (Thermo Fisher Scientific, Waltham, MA, USA) and incubated for 5 min at 25 °C. A total of 8 μL of Lipofectamine 2000 (Invitrogen, Carlsbad, CA, USA) was diluted in 250 μL of opti-MEM and then mixed with diluted DNA after 5 min incubation at 25 °C at a final volume of 500 μL. The medium was replaced with 500 μL opti-MEM 30 min before transfection, and the mixture was incubated for 25 min at 25 °C, followed by addition to glass bottom cell culture dish (MatTek Corporation, MA, USA).

### 2.2. Polyclonal antibodies

The DNA-launched infectious clone (Chen et al., 2017) was used to amplify the 3D fragment with primers pET-32a-3D-F/R (Table 1). The fragment was digested with *Bam*H I and *Xho* I and then were inserted into pET-32a(+) vector (Novagen, Darmstadt, Germany) to establish pET-32a-3D. The protein (named 3D-fusion protein) was expressed in *E. coli* Rosetta (DE3) cells (Transgen Biotech, Beijing, China) after 3 h induction with 1 mM IPTG at 37 °C. The 3D genome length is 1359 bp, which expresses a 66.4 kDa fusion protein (Zhang et al., 2017). The recombinant proteins were purified by eluting from SDS-PAGE as previously described (Zhang et al., 2012). In brief, inclusion body proteins were separated by SDS-PAGE, the proteins of interest were excised, and the gel slices were crushed and added to an appropriate volume of sterilized PBS. After several cycles of freeze-thawing, the fusion proteins were dissolved in PBS, and the PBS was separated from the solid gel by centrifugation. The purified protein was then used to produce polyclonal antibodies. Female six-week-old BALB/c mice were primed subcutaneously with purified 3D-fusion protein emulsified with an equal volume of Freund's complete adjuvant (Sigma-Aldrich, St. Louis, MO, USA). Two booster immunizations were given at two weeks intervals with the 3D-fusion protein in Freund's incomplete adjuvant. The purified 3D-fusion protein without adjuvant was injected intraperitoneally as the final immunization. The mice were euthanized 72 h later, and the collected polyclonal antisera (named $3D^{pol}$-antisera) were used to measure the cellular localization of $3D^{pol}$.

**Table 1**
Primers that used in this research.

| Primer | Primer sequences (5'→3') |
|---|---|
| pET-32a-3D-F | GGA TCC GGG AAA GTA GTA AGC AAG CAA TA |
| pET-32a-3D-R | CTC GAG TTA GAT CAT CAT GCA AGC TGT GTA TGC |
| pcDNA-3CD-F | GGA TCC AGC GGG CGG GTG AAT TTC AGA CAT |
| pcDNA-3CD-R | CTC GAG TTA GAT CAT CAT GCA AGC TGT GTA TGC |
| RT-qPCR-F | AGA CAC ATG TTG CTG AAA AAC T |
| RT-qPCR-R | AGA ACC AGT TGT CGT TTG GTC |
| DHAV-1-Probe | Cy5-ATG CCA TGA CAC TAT CTC ATA TGA GTC AGC-BHQ-2 |

### 2.3. Plasmids construction

The fragment 3D was then inserted into pcDNA™3.1/V5-His A vector (Novagen) after digestion with *Bam*H I and *Xho* I to establish the recombinant plasmid pcDNA-3D, and the expressed proteins were named $3D^{pol}$. The fragment 3CD was amplified with primers pcDNA-3CD-F/R (Table 1). The fragments were digested with *Bam*H I and *Xho* I and then were inserted into pcDNA™3.1/V5-His A vector to establish the recombinant plasmid pcDNA-3CD. The 3CD genome length is 1902 bp, which expresses an 86.1 kDa protein named 3CD (estimate by DNA Star LaserGene software, DNAStar Inc. Madison, WI). The amino acid sequence $^{17}$PRKTAYMRS$^{25}$ of $3D^{pol}$/3CD was removed to establish recombinant plasmids pcDNA-3D-Δ17-25 or pcDNA-3CD-Δ17-25, and the expression products were named $3D^{pol}$-Δ17-25 or 3CD-Δ17-25, respectively. The $^{18}$R, $^{19}$K and $^{24}$R of pcDNA-3D were mutated into $^{18}$A, $^{19}$A and $^{24}$A respectively to establish pcDNA-3D-18A, pcDNA-3D-19A and pcDNA-3D-24A, and the expression products were named $3D^{pol}$-18A, $3D^{pol}$-19A and $3D^{pol}$-24A respectively. The recombinant plasmid pcDNA-3D-$^{24}$K was constructed based on pcDNA-3D by mutating $^{24}$R into $^{24}$K. The complete 3D fragment of strain ABL96623 with mutation from $^{24}$K to $^{24}$R were synthesized by Sangon Biotech (Shanghai, China) and then were inserted into pcDNA™3.1/V5-His A vector to establish pcDNA-ABL9662-$^{24}$R (Fig. 2A).

### 2.4. Western blot

Cell lysates were subjected to SDS-PAGE on a 12% polyacrylamide gel, and the separated proteins were electroblotted onto a polyvinylidene fluoride (PVDF) membrane (Thermo Fisher Scientific) using transfer buffer MT (25 mM Tris, pH 8.0, 0.19 M glycine, 20% methanol). Thereafter, the PVDF membrane was blocked with 5% non-fat milk in Tris-buffered saline with Tween 20 (TBST, 500 ml NaCl, 0.05% Tween 20, 10 mM TRIS-HCl, pH 7.5) for 1 h at room temperature. Next, the membrane was incubated with $3D^{pol}$-antisera (1:100) or anti His-tag mouse monoclonal antibody (mAb) (GEHealthcare Life Science, Pittsburgh, USA, 1:3000) at 4 °C for 8 h. The membrane was washed for four times with TBST and incubated with a horseradish peroxidase (HRP)-conjugated goat anti-mouse antibody (1:3000; Abcam) at 4 °C for 4 h. The PVDF membrane was rinsed with TBST for 5 times, developed with hydrogen peroxide and 3,3′-diaminobenzidine tetrahydrochloride (Sigma), and then visualized with the enhanced chemiluminescence system (Bio-Rad, USA).

### 2.5. Quantitative (q)RT-PCR

The viral RNA copy number was quantified by RT-qPCR as previously described (Lin et al., 2016). The viral RNA was extracted with

E.Z.N.A.TM Viral RNA Kit (Omega Bio-Tek, Norcross, GA, USA) according to the manufacturer's instruction. Using the primers RT-qPCR-F/R and the DHAV-1-Probe (Table 1), a TaqMan real-time RT-PCR assay for quantitative detection of DHAV-1 was conducted in a total volume of 25 μL and containing 12.5 μL 2 × One-step RT-qPCR buffer (with ROX), 0.4 μM of forward and reverse primers, 0.2 μM of the probe, 0.9 μL EnzyMix, and 2 μL of template RNA. The reaction cycles were as follows: 95 °C denaturation for 5 min, followed by 40 cycles at 95 °C for 15 s, annealing at 60 °C for 45 s, with fluorescence measured at every annealing step. Non-template control samples were included in each reaction. Viral RNA copies were calculated using the formula $X = 6.7 \times 10^{(40.812-y)/3.285}$, where X represents a standard of viral copies, and y represents a standard of values derived from one-step real-time PCR.

### 2.6. Laser scanning confocal microscopy (LSCM)

Cells were seeded into dishes and grown to 70%–80% confluence, and then were transfected with the recombinant plasmids. The transfected cells were washed for five times with PBS at 24 h post transfection (hpt), fixed by a mixture of acetone and formaldehyde (1:1) for 8 min at room temperature. The samples were then incubated with $3D^{pol}$-antisera for 1 h at 37 °C. Cells were then rinsed with TBST for 5 times and then incubated with FITC-conjugated goat anti-mouse antibody (Abcam, 1:3000). The samples were washed with PBS, inoculated with 500 μL DAPI (4′,6-diamidino-2-phenylindole) for 15 min. After washing for five times with PBS, samples were then imaged with a laser confocal microscope (Leica AF6000). Images were obtained in double excitation mode and were processed using Adobe Photoshop.

## 3. Results

### 3.1. The $3D^{pol}$-antisera specifically recognized 3D-fusion protein

To measure the cellular localization of $3D^{pol}$ during DHAV-1 propagation, the recombinant plasmid pET-32a-3D was established to obtain the anti-3D-fusion polyclonal antisera (named $3D^{pol}$-antisera). Equal volume of the 3D-fusion protein was subjected to electrophoresis on 12% denaturing SDS-PAGE, following with the western blot analysis with $3D^{pol}$-antisera or anti His-tag mouse mAb. The results showed that 3D-fusion protein was about 66.4 kDa, and both the $3D^{pol}$-antisera (Fig. 1A) and anti His-tag mouse mAb (Fig. 1B) specifically recognized

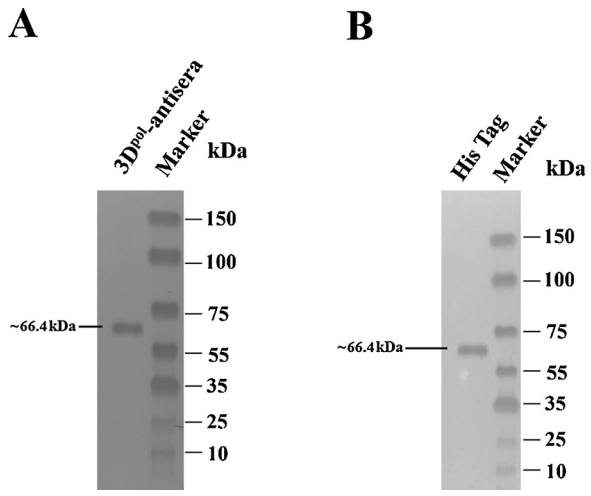


**Fig. 1.** Both the $3D^{pol}$-antisera and anti-His antibody specifically recognized 3D-fusion protein. Equal volume of 3D-fusion protein was run on 12% denaturing SDS-PAGE. The separated proteins were conducted with western blot analysis with (**A**) $3D^{pol}$-antisera (1:100) or (**B**) anti His-tag mouse mAb (1:3000).

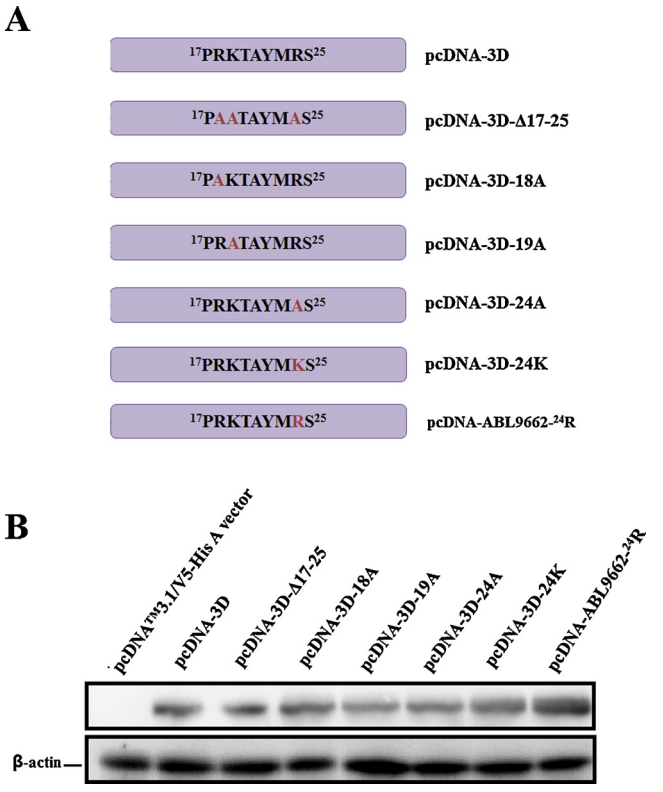


**Fig. 2.** 3D protein expression. (**A**) Construction of 3D recombinant plasmids. (**B**) 4.0 μg of recombinant plasmids were transfected in to DEFs, cell lysates were collected and used for western blot analysis with $3D^{pol}$-antisera (1:100) and HRP-conjugated goat anti-mouse antibody (1:3000) at 24 hpt. Same copies of pcDNA™3.1/V5-His A vector were also transfected into DEFs as control.

3D-fusion protein.

### 3.2. Expression of 3D polypeptides

To explore the cellular localization of $3D^{pol}$ during viral propagation, a series of constructs were established (Fig. 2A). The recombinant plasmids pcDNA-3D, pcDNA-3D-Δ17-25, pcDNA-3D-18A, pcDNA-3D-19A, pcDNA-3D-24A, pcDNA-3D-24 K and pcDNA-ABL9662-$^{24}$R were transfected into DEFs, respectively. Same copies of pcDNA™3.1/V5-His A vector were transfected into DEFs to serve as negative control. Cell lysates from those transfection groups were collected at 24 hpt to perform western blot analysis with $3D^{pol}$-antisera. The results showed that proteins were highly expressed in each transfection group (Fig. 2B).

### 3.3. $3D^{pol}$ and 3CD entered into nucleus during viral propagation

DEFs were infected with $10^{5.0}$ copies (measured by RT-qPCR) of DHAV-1 strain LY0801. At 24 h post infection (hpi), the cellular localization of $3D^{pol}$/3CD was measured through LSCM with $3D^{pol}$-antisera and FITC-conjugated goat anti-mouse antibody. The LSCM results showed that $3D^{pol}$/3CD localized in both nucleus and cytoplasm (Fig. 3A), indicating that $3D^{pol}$/3CD possessed nuclear targeting activity. Blank DEFs were also conducted with LSCM assay under same condition to serve as control, and no fluorescence was detected (Fig. 3B). Based on that, the cellular localization of 3CD was measured by transfecting recombinant plasmid pcDNA-3CD into DEFs. Western blot results showed that 3CD was highly expressed (Fig. 3E), and $3D^{pol}$/3CD could also enter into nucleus (Fig. 3C). pcDNA™3.1/V5-His A vector was transfected into DEFs as negative control (Fig. 3D).The collected data indicated that both $3D^{pol}$ and 3CD possessed nuclear targeting activities.

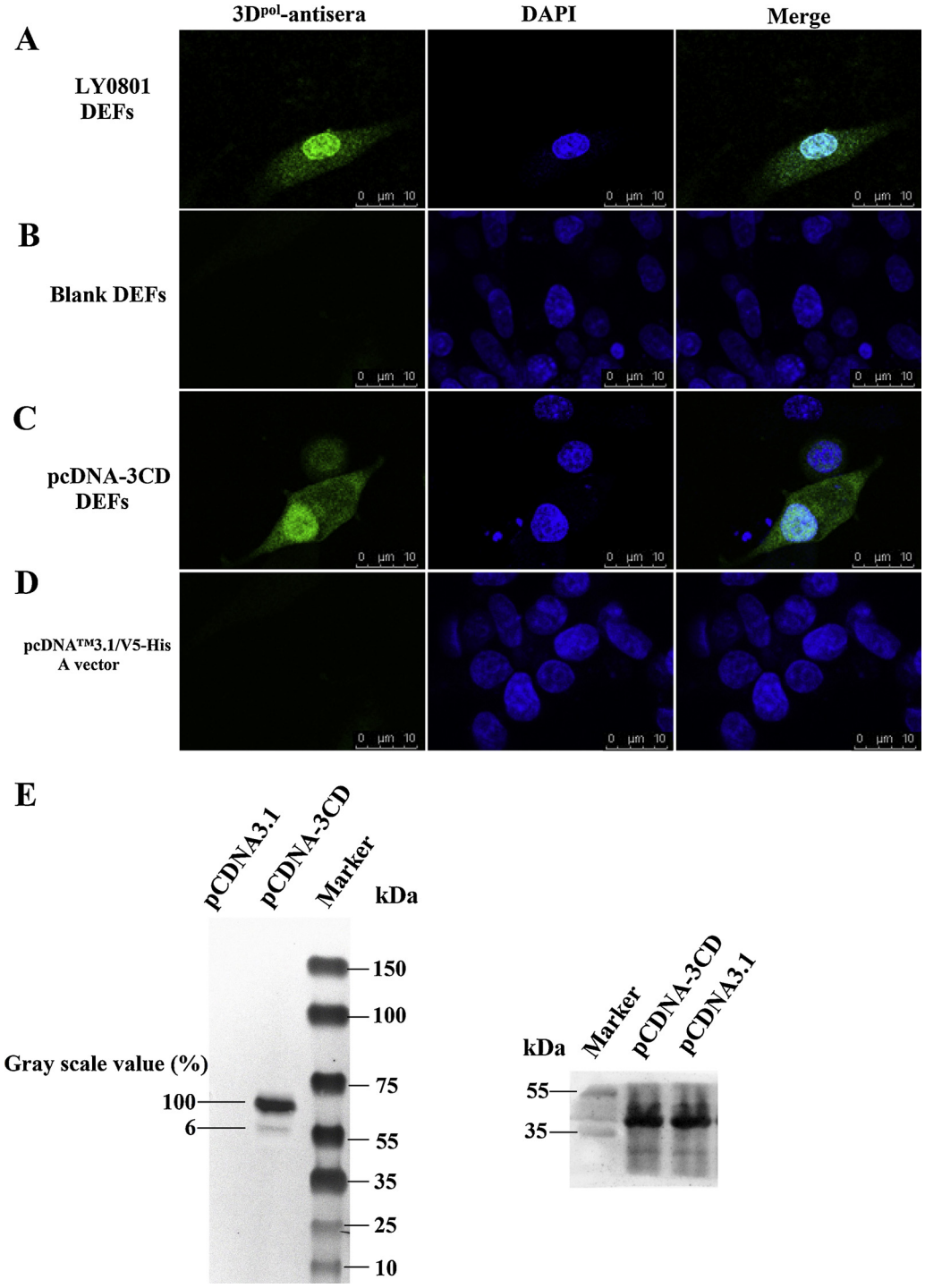


**Fig. 3.** $3D^{pol}$ and 3CD entered into nucleus during viral propagation. (**A**) DEFs were seeded into glass bottom cell culture dish and grown to 70% confluence, following with infection with DHAV-1. At 24 hpi, the samples were imaged with laser confocal microscope as previously described. (**B**) LSCM assay was conducted in blank DEFs with $3D^{pol}$-antisera (1:100) and FITC-conjugated goat anti-mouse antibody (Abcam, 1:3000) at 24 hpt. (**C**) 4.0 μg of the recombinant plasmids pcDNA-3CD was transfected into DEFs, the LSCM assay was conducted at 24 hpt as previously described. Bars represent 10 μm. (**D**) Same copies of pcDNA™3.1/V5-His A vector was transfected into DEFs as negative control. (**E**) DEFs transfected with 4.0 μg of the recombinant plasmids pcDNA-3CD was analyzed with western blot with $3D^{pol}$-antisera (1:100) and HRP-conjugated goat anti-mouse antibody (1:3000).

### *3.4. $^{17}$PRKTAYMRS$^{25}$ was a functional NLS*

Next, the cellular localization of $3D^{pol}$ in eukaryotic expression system was measured through transfecting the recombinant plasmid pcDNA-3D into DEFs. At 24 hpt, the samples were imaged, and the results showed that $3D^{pol}$ could enter into the nucleus of DEFs (Fig. 4A). In order to confirm whether the cellular localization of $3D^{pol}$ of DHAV-1 was cell-line-specific, pcDNA-3D was also transfected into BHK-21 cells and CHO cell line respectively. The results showed that $3D^{pol}$ could also enter into nucleus of BHK-21 cells (Fig. 4B) and CHO (Fig. 4C). Same copies of pcDNA™3.1/V5-His A vector were transfected into DEFs to serve as negative control, and no fluorescence was observed (Fig. 4D).

To further explore the exact mechanism by which $3D^{pol}$/3CD enters into nucleus, the amino sequences of 3CD were analyzed through NLS Mapper program. The predicted results showed that $3D^{pol}$ possesses a NLS $^{17}$PRKTAYMRS$^{25}$. The plasmid pcDNA-3D-Δ17-25 and pcDNA-3CD-Δ17-25 was then transfected into DEFs to identify whether the $^{17}$PRKTAYMRS$^{25}$ was a functional NLS. The LSCM results showed that $3D^{pol}$-Δ17-25 and 3CD-Δ17-25 localized exclusively in the cytoplasm (Fig. 4E, F). Western blot results showed that $3D^{pol}$/3CD and $3D^{pol}$/3CD-Δ17-25 were highly expressed in each group (Fig. 4G). These results indicated that $^{17}$PRKTAYMRS$^{25}$ was a functional NLS to guide $3D^{pol}$/3CD into nucleus.

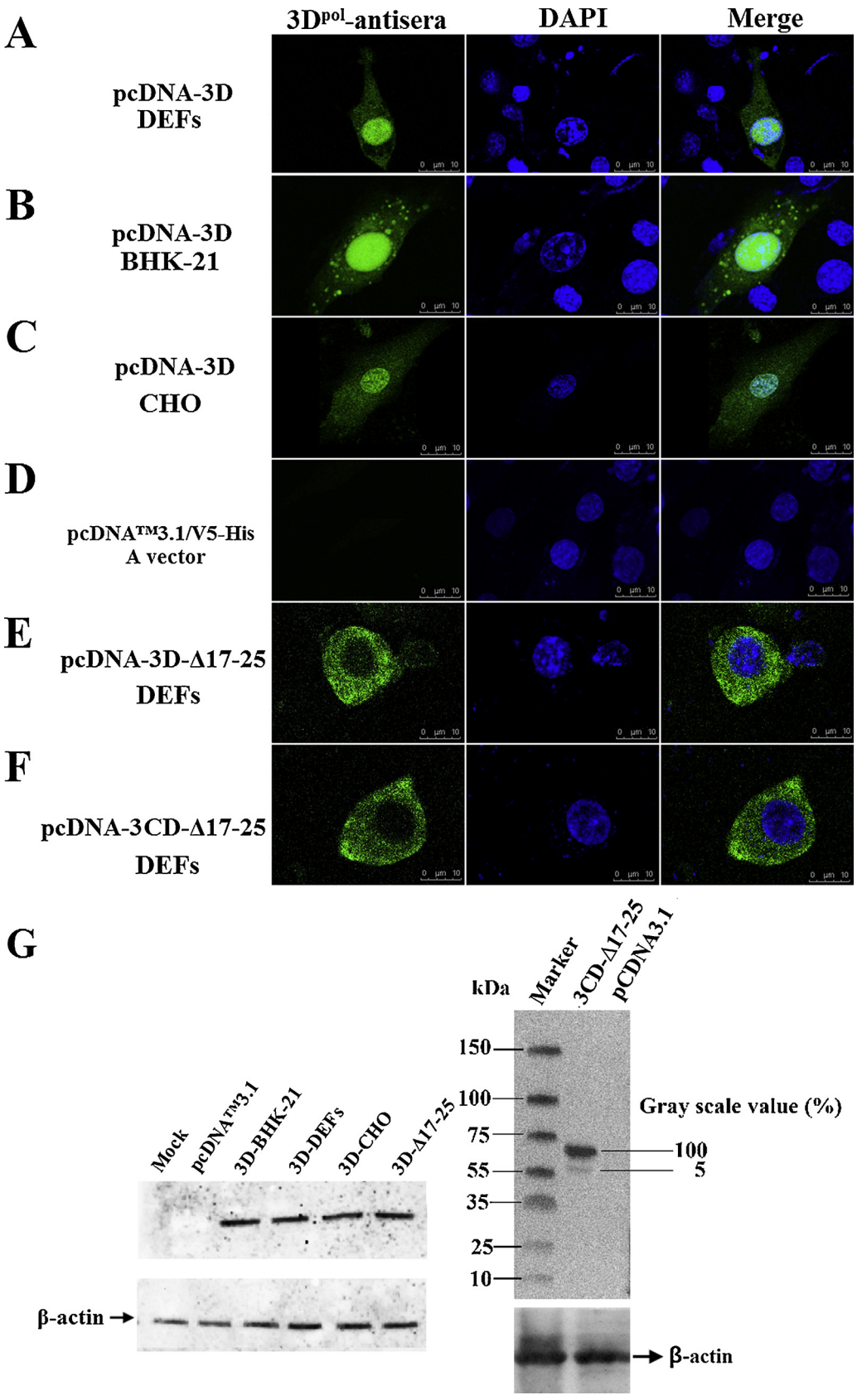


**Fig. 4.** The amino acid motif $^{17}$PRKT-AYMRS$^{25}$ of DHAV-1 3D$^{pol}$/3CD was identified as a functional NLS. The recombinant plasmid pcDNA-3D was transfected into DEFs (**A**), BHK-21 cells (**B**), and CHO cells (**C**), and cellular localization of the 3D$^{pol}$ was measured at 24 hpt, respectively. (**D**) LSCM assay was conducted in DEFs transfected with same copies of pcDNA™3.1/V5-His A vector as previously describes. The plasmids pcDNA-3D-Δ17-25 (**E**) and pcDNA-3CD-Δ17-25 (**F**) were transfected into DEFs, and the cellular localization of 3D$^{pol}$ absent of $^{17}$PRKT-AYMRS$^{25}$ was measured at 24 hpt, respectively. Bars represent 10 μm. (**G**) The DEFs in each transfected group were collected at 24 hpt to conduct western blot analysis with 3D$^{pol}$-antisera (1:100) and HRP-conjugated goat anti-mouse antibody (1:3000).

### 3.5. Identification of the key residues in the functional NLS

In order to measure the vital basic amino acids in its nuclear localization signal, site-directed mutagenesis was used to construct a series of mutants (Fig. 2A). The $^{18}$R, $^{19}$K and $^{24}$R of DHAV-1 3D$^{pol}$ were replaced by Ala, respectively. The corresponding plasmids were transfected into DEFs, and the samples were imaged at 24 hpt. The 3D$^{pol}$-18A, 3D$^{pol}$-19A and 3D$^{pol}$-24A proteins were observed localizing in the

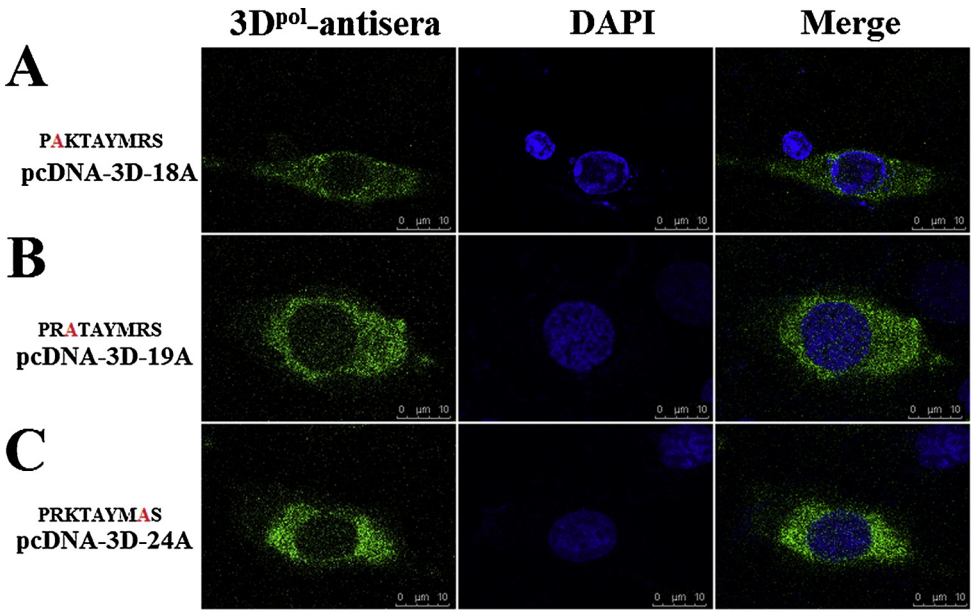


D

| Strain | Accession no. | Amino acid sequence |
|---|---|---|
| DHAV-1 | FJ436047 | PRKTAYMRS |
| DHAV-1 | KX242347 | PRKTAYMRS |
| DHAV-1 | ABL96623 | PRKTAYMRS |
| DHAV-1 | ABB22724 | PRKTAYMRS |
| DHAV-1 | AHJ78642 | PRKTAYMRS |
| DHAV-1 | ACJ63291 | PRKTAYMRS |

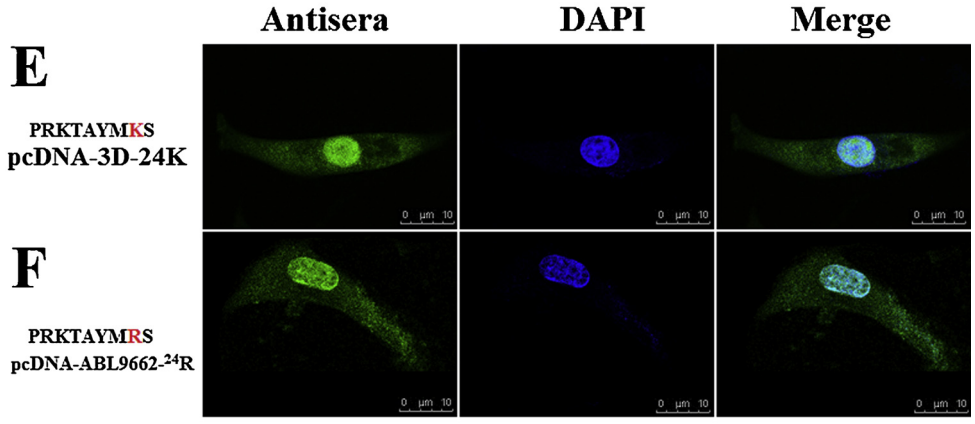


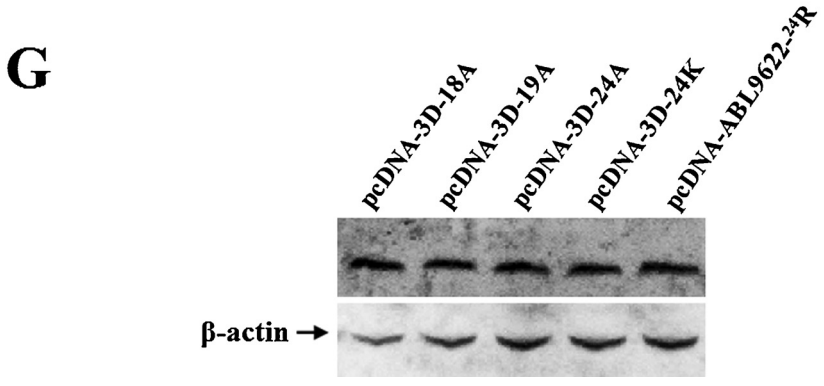


**Fig. 5.** Identification of the key residues in the amino acid motif $^{17}$PRKTAYMRS$^{25}$ of DHAV-1 3D$^{pol}$/3CD. The plasmids pcDNA-3D-18A ($^{18}$R changed to $^{18}$A) (**A**), pcDNA-3D-19A ($^{19}$K changed to $^{19}$A) (**B**), pcDNA-3D-24A ($^{24}$R changed to $^{24}$A) (**C**) were transfected into DEFsrespectively to measure cellular localization of the mutated 3D$^{pol}$ at 24 hpt. (**D**) Alignment of the amino acid sequences corresponding to the 3D$^{pol}$ of DHAV-1 strains. The plasmids pcDNA-3D-24 K ($^{24}$R changed to $^{24}$K) (**E**) andpcDNA-ABL9662-$^{24}$R ($^{24}$K changed to $^{24}$R) (**F**) were transfected into DEFs respectively to measure cellular localization of the 3D$^{pol}$ at 24 hpt. Bars represent 10 μm. (**G**) Cell lysates in each group were collected at 24 hpt and used for western blot analysis with 3D$^{pol}$-antisera (1:100) and HRP-conjugated goat anti-mouse antibody (1:3000).

cytoplasm of the transfected cells (Fig. 5A–C). The results suggested that $^{18}$R, $^{19}$K and $^{24}$R were essential for maintaining the nuclear targeting activity of the DHAV-1 3D$^{pol}$.

The sequence analysis result showed that the amino acid $^{24}$R of 3D$^{pol}$ was replaced by $^{24}$K in some other DHAV-1 strains. The DHAV-1 strains with amino acid $^{24}$R of 3D$^{pol}$ were listed in Fig. 5D, and the remaining strains in GenBank possessed $^{24}$K in 3D$^{pol}$. In order to measure whether the mutation from $^{24}$R to $^{24}$K affected the function of NLS, the amino acid $^{24}$R was changed to $^{24}$K in the 3D$^{pol}$ of LY0801 strain, meanwhile the amino acid $^{24}$K was changed to $^{24}$R in the 3D$^{pol}$ of ABL9662 strain. The two recombinant plasmids pcDNA-3D-24 K and pcDNA-ABL9662-$^{24}$R were transfected into DEFs. At 24 hpt, the two mutated 3D$^{pol}$ proteins were observed localizing in the nucleus of the transfected cells (Fig. 5E, F). These results indicated that exchanging between $^{24}$R and $^{24}$K had no impact on the nuclear targeting activity of the DHAV-1 3D$^{pol}$.

## 4. Discussion

As obligate intracellular pathogens, viruses exploit the host translational machinery to generate viral proteins. For some picornaviruses, viral infection can cause inhibition of nuclear-cytoplasmic trafficking leading to accumulation of nuclear proteins in the cytoplasm (Belov et al., 2000; Gustin and Sarnow, 2001, 2002). Some nuclear proteins, such as La autoantigen, Sam 68, and nucleolin, accumulate in the cytoplasm and interacted with viral genome and proteins of PV (McBride et al., 1996; Meerovitch et al., 1993; Waggoner and Sarnow, 1998). However, as the major target for protease 3C of picornaviruses, the TATA-binding protein (TBP) was found not to relocalize to the cytoplasm of infected cells (Gustin and Sarnow, 2001). The inability of TBP to be translocated to the cytoplasm of infected cells necessitated 3C, 3CD or some other 3C-containing precursor entering into the nucleus and subsequent cleavage of TBP leading to shut-off of host cell transcription (Sharma et al., 2004). Although the cellular proteins accumulate in the infected cell cytoplasm, the viral proteins (3D$^{pol}$/3CD) are capable of moving in the opposite direction in a NLS-dependent fashion. Therefore, the entry of 3CD or 3D$^{pol}$ into nucleus might be essential for shutoff of host cell transcription and maintaining the viral propagation of DHAV-1.

Although it has been demonstrated that 3D$^{pol}$ played an important role in DHAV-1 replication by acting as an RdRP (Zhang et al., 2017), the replication mechanism of DHAV-1 was still unclear. In this research, 3D$^{pol}$/3CD was found entering into nucleus during viral propagation (Fig. 3). To explore how 3D$^{pol}$/3CD entered into nucleus, the 3CD sequence was analyzed through the online computer program NLS Mapper, and the predicted result showed that the amino acid sequence $^{17}$PRKTAYMRS$^{25}$ in 3D$^{pol}$ might be a NLS. The DHAV-1 3D$^{pol}$/3CD absent of the amino acid sequence $^{17}$PRKTAYMRS$^{25}$ was observed only localizing in cytoplasm, indicating that $^{17}$PRKTAYMRS$^{25}$ was a functional NLS. Besides, $^{18}$R, $^{19}$K and $^{24}$R were found essential for maintaining the nuclear targeting activities, yet exchange between $^{24}$R and $^{24}$K had no impact on nuclear targeting activities. Further investigation should be conducted to reveal how the entry of 3CD or 3D$^{pol}$ into nucleus shutoff cellular transcription and maintain the efficient viral replication of DHAV-1.

The active transport of macromolecules between nucleus and cytoplasm is an energy dependent process that requires the involvement of receptor proteins, named importins or exportins, which recognize specific amino acid sequences in the cargos to promote transport through the nuclear pores (Alves et al., 2008; Pemberton and Paschal, 2005; Stewart, 2007). The NLS is exposed on the surface of the virion and is thus capable of interacting with a putative NLS receptor (Leclerc et al., 1999). To picornaviruses, such as foot-and-mouth disease virus (FMDV) and PV, the nuclear localization of the 3D has been identified (Amineva et al., 2004; García-Briones et al., 2006; Sanchez-Aparicio et al., 2013; Sharma et al., 2004; Weidman et al., 2003). The 3D$^{pol}$ of DHAV-1 located in the nucleus, suggesting that 3D$^{pol}$ contains one or more functional NLSs which are responsible for the delivery of 3D$^{pol}$ into the nucleus. In this research, one putative NLS was found at the N terminus of the 3D$^{pol}$ of DHAV-1 through the online computer program NLS Mapper. In order to characterize whether the NLS was functional, the cellular localization of truncated 3D$^{pol}$/3CD with/without the amino acid sequence $^{17}$PRKTAYMRS$^{25}$ was measured, and the result showed that $^{17}$PRKTAYMRS$^{25}$ was the key factor for maintaining the nuclear targeting activities (Fig. 4). The functional NLS $^{17}$PRKTAYMRS$^{25}$ in 3D$^{pol}$ was quite similar to the functional NLS $^{15}$PRKTALRPT$^{23}$ in EMCV (accession no. L22089) (Aminev et al., 2003). In this research, we noticed that a small amount of 3D was detected in pCDNA-3CD transfection group (Fig. 3E and 4 G). Although we have no specific data to show how 3D come from, we assumed that the 3CD partial positive results of LSCM should be contributed by the 3D NLS.

The basic amino acids play an important role in the NLS of viral proteins (Nigg, 1997; Terry et al., 2007). The NLS motif $^{16}$MRKTKLAPT$^{24}$ of 3D$^{pol}$ protein was conserved in all the 7 different serotypes of FMDV (Carrillo et al., 2005). The mutations $^{18}$K→$^{18}$E and $^{20}$K→$^{20}$E in NLS could result in decrease on both the nuclear targeting ability of 3D$^{pol}$/3CD and viral infectivity of FMDV (Sanchez-Aparicio et al., 2013). In PV-infected cells, mutations from $^{125}$KKK$^{127}$ to $^{125}$AAA$^{127}$ in NLS interfered in the nuclear entrance of 3D$^{pol}$/3CD (Sharma et al., 2004). In this study, we found that the mutations $^{18}$R→$^{18}$A, $^{19}$K→$^{19}$A, and $^{24}$R→$^{24}$A completely abrogated the function of nuclear localization respectively, but the exchange between $^{24}$R and $^{24}$K had no impact on the nuclear localization activity (Fig. 5). These results suggested that $^{18}$R, $^{19}$K and $^{24}$R were vital for translocation of 3D$^{pol}$ of DHAV-1, and the amino acid $^{24}$R of 3D$^{pol}$ replaced by $^{24}$K in some other DHAV-1 strains should not affect the viral replication.

Based on the data, it can be said that a portion of life cycle of a cytoplasmic RNA virus does include interaction with the host cell nucleus, and the conserved NLS might play important role to relocate some certain viral proteins and could be essential for efficient viral replication in the host cells. Further investigation of whether there was other putative NLS in viral proteins will be conducted to understand how and why cytoplasmic RNA viruses interact with the nuclei.

In conclusion, we investigated that 3D$^{pol}$/3CD entered into nucleus during viral propagation of DHAV-1. The amino acid $^{17}$PRKTAYMRS$^{25}$ in 3D$^{pol}$ was proved to be a functional NLS to guide 3D$^{pol}$/3CD into nucleus, and $^{18}$R, $^{19}$K and $^{24}$R in the NLS were found essential for maintaining nuclear targeting activity of the protein.

## Acknowledgements

This work was supported by the National Key Research and Development Program of China (2017YFD0500800); the National Natural Science Foundation of China (31772754); Shandong Modern Agricultural Technology & Industry System, China (SDAIT-11-15); Funds of Shandong “Double Tops” Program, China (SYL2017YSTD11).

## References

Aminev, A.G., Amineva, S.P., Palmenberg, A.C., 2003. Encephalomyocarditis virus (EMCV) proteins 2A and 3BCD localize to nuclei and inhibit cellular mRNA transcription but not rRNA transcription. Virus Res. 95 (1–2), 59–73.

Alves, C., Freitas, N., Cunha, C., 2008. Characterization of the nuclear localization signal of the hepatitis delta virus antigen. Virology 370 (1), 12–21.

Amineva, S.P., Aminev, A.G., Palmenberg, A.C., Gern, J.E., 2004. Rhinovirus 3C protease precursors 3CD and 3CD' localize to the nuclei of infected cells. J. Gen. Virol. 85 (Pt 10), 2969–2979.

Belov, G.A., Evstafieva, A.G., Rubtsov, Y.P., Mikitas, O.V., Vartapetian, A.B., Agol, V.I., 2000. Early alteration of nucleocytoplasmic traffic induced by some RNA viruses. Virology 275, 244–248.

Carrillo, C., Tulman, E.R., Delhon, G., Lu, Z., Carreno, A., Vagnozzi, A., Kutish, G.F., Rock, D.L., 2005. Comparative genomics of foot-and-mouth disease virus. J. Virol. 79 (10), 6487–6504.

Chen, J., Zhang, R., Lin, S., Li, P., Lan, J., Xie, Z., Wang, Y., Jiang, S., 2017. Construction and characterization of an improved DNA-launched infectious clone of duck hepatitis

a virus type 1. Virol. J. 14 (1), 212.
Colpitts, T.M., Barthel, S., Wang, P., Fikrig, E., 2011. Dengue virus capsid protein binds core histones and inhibits nucleosome formation in human liver cells. PLoS One 6 (9), e24365.
Gao, J., Chen, J., Si, X., Xie, Z., Zhu, Y., Zhang, X., Wang, S., Jiang, S., 2012. Genetic variation of the VP1 gene of the virulent duck hepatitis A virus type 1 (DHAV-1) isolates in Shandong province of China. Virol. Sin. 27 (4), 248–253.
García-Briones, M., Rosas, M.F., González-Magaldi, M., Martín-Acebes, M.A., Sobrino, F., Armas-Portela, R., 2006. Differential distribution of non-structural proteins of foot-and-mouth disease virus in BHK-21 cells. Virology 349 (2), 409–421.
Goldfarb, D.S., Corbett, A.H., Mason, D.A., Harreman, M.T., Adam, S.A., 2004. Importin alpha: a multipurpose nuclear-transport receptor. Trends Cell Biol. 14 (9), 505–514.
Gong, P., Peersen, O.B., 2010. Structural basis for active site closure by the poliovirus RNA-dependent RNA polymerase. Proc. Natl. Acad. Sci. U. S. A. 107 (52), 22505–22510.
Gorlich, D., Mattaj, I.W., 1996. Nucleocytoplasmic transport. Science 271 (5255), 1513–1518.
Gustin, K.E., Sarnow, P., 2001. Effects of poliovirus infection on nucleocytoplasmic trafficking and nuclear pore complex composition. EMBO J. 20, 240–249.
Gustin, K.E., Sarnow, P., 2002. Inhibition of nuclear import and alteration of nuclear pore complex formation by rhinovirus. J. Virol. 76, 8787–8796.
Haider, S.A., Calnek, B.W., 1979. In vitro isolation, propagation, and characterization of duck hepatitis virus type III. Avian Dis. 23 (3), 715–729.
Guo, Y.P., Pan, W.S., 1984. Preliminary identifications of the duck hepatitis virus serotypes isolated in Beijing. China J. Vet. Med. 10, 2–3 (in Chinese).
Kim, M.C., Kwon, Y.K., Joh, S.J., Lindberg, A.M., Kwon, J.H., Kim, J.H., Kim, S.J., 2006. Molecular analysis of duck hepatitis virus type 1 reveals a novel lineage close to the genus Parechovirus in the family Picornaviridae. J. Gen. Virol. 87 (Pt 11), 3307–3316.
Kim, M.C., Kwon, Y.K., Joh, S.J., Kim, S.J., Tolf, C., Kim, J.H., Sung, H.W., Lindberg, A.M., Kwon, J.H., 2007. Recent Korean isolates of duck hepatitis virus reveal the presence of a new geno- and serotype when compared to duck hepatitis virus type 1 type strains. Arch. Virol. 152 (11), 2059–2072.
Knowles, N.J., Hovi, T., Hyypiä, T., King, A.M.Q., Lindberg, A.M., Pallansch, M.A., Palmenberg, A.C., Simmonds, P., Skern, T., Stanway, G., Yamashita, T., Zell, R., 2012. Picornaviridae. In: King, A.M.Q., Adams, M.J., Carstens, E.B., Lefkowitz, E.J. (Eds.), Virus Taxonomy. Classification and Nomenclature of Viruses: Ninth Report of the International COmmittee on Taxonomy of Viruses. Elsevier Academic Press, San Diego, CA, USA, pp. 855–880.
Leclerc, D., Chapdelaine, Y., Hohn, T., 1999. Nuclear targeting of the cauliflower mosaic virus coat protein. J. Virol. 73 (1), 553–560.
Levine, P., Fabricant, J., 1950. A hitherto-undescribed virus disease of ducks in North America. Cornell Vet. 40, 71–86.
Lin, S.L., Cong, R.C., Zhang, R.H., Chen, J.H., Xia, L.L., Xie, Z.J., Wang, Y., Zhu, Y.L., Jiang, S.J., 2016. Circulation and in vivo distribution of duck hepatitis A virus types 1 and 3 in infected ducklings. Arch. Virol. 161 (2), 405–416.
Marcotte, L.L., Wass, A.B., Gohara, D.W., Pathak, H.B., Arnold, J.J., Filman, D.J., Cameron, C.E., Hogle, J.M., 2007. Crystal structure of poliovirus 3CD protein: virally encoded protease and precursor to the RNA-dependent RNA polymerase. J. Virol. 81 (7), 3583–3596.
Meerovitch, K., Svitkin, Y.V., Lee, H.S., Lezbkowicz, F., Kenan, D.J., Chan, E.K., Agol, V.I., Keene, J.D., Sonenberg, N., 1993. La autoantigen enhances and corrects aberrant translation of poliovirus RNA in reticulocyte lysate. J. Virol. 67, 3798–3807.
Sanchez-Aparicio, M.T., Rosas, M.F., Sobrino, F., 2013. Characterization of a nuclear localization signal in the foot-and-mouth disease virus polymerase. Virology 444 (1–2), 203–210.
McBride, A.E., Schlegel, A., Kirkegaard, K., 1996. Human protein Sam68 relocalization and interaction with poliovirus RNA polymerase in infected cells. Proc. Natl. Acad. Sci. U. S. A. 93, 2296–2301.
McLane, L.M., Corbett, A.H., 2009. Nuclear localization signals and human disease. IUBMB Life 61 (7), 697–706.
Nguyen, H.T., Chong, Y., Oh, D.K., Heo, Y.S., Viet, P.T., Kang, L.W., Jeon, S.J., Kim, D.E., 2013. An efficient colorimetric assay for RNA synthesis by viral RNA-dependent RNA polymerases, using thermostable pyrophosphatase. Anal. Biochem. 434 (2), 284–286.
Nigg, E.A., 1997. Nucleocytoplasmic transport: signals, mechanisms and regulation. Nature 386 (6627), 779–787.
Pei, Y., Hodgins, D.C., Lee, C., Calvert, J.G., Welch, S.K., Jolie, R., Keith, M., Yoo, D., 2008. Functional mapping of the porcine reproductive and respiratory syndrome virus capsid protein nuclear localization signal and its pathogenic association. Virus Res. 135 (1), 107–114.
Pemberton, L.F., Paschal, B.M., 2005. Mechanisms of receptor-mediated nuclear import and nuclear export. Traffic 6 (3), 187–198.
Sharma, R., Raychaudhuri, S., Dasgupta, A., 2004. Nuclear entry of poliovirus protease-polymerase precursor 3CD: implications for host cell transcription shut-off. Virology 320 (2), 195–205.
Shatskaya, G.S., Drutsa, V.L., Koroleva, O.N., Osterman, I.A., Dmitrieva, T.M., 2013. Investigation of activity of recombinant mengovirus RNA-dependent RNA polymerase and its mutants. Biochemistry (Mosc.) 78 (1), 96–101.
Sierra, M., Airaksinen, A., Gonzalez-Lopez, C., Agudo, R., Arias, A., Domingo, E., 2007. Foot-and-mouth disease virus mutant with decreased sensitivity to ribavirin: implications for error catastrophe. J. Virol. 81 (4), 2012–2024.
Stewart, M., 2007. Molecular mechanism of the nuclear protein import cycle. Nat. Rev. Mol. Cell Biol. 8 (3), 195–208.
Terry, L.J., Shows, E.B., Wente, S.R., 2007. Crossing the nuclear envelope: hierarchical regulation of nucleocytoplasmic transport. Science 318 (5855), 1412–1416.
Toth, T.E., 1969. Studies of an agent causing mortality among ducklings immune to duck virus hepatitis. Avian Dis. 13 (4), 834–846.
Tseng, C.H., Tsai, H.J., 2007. Molecular characterization of a new serotype of duck hepatitis virus. Virus Res. 126, 19–31.
Walker, E., Jensen, L., Croft, S., Wei, K., Fulcher, A.J., Jans, D.A., Ghildyal, R., 2016. Rhinovirus 16 2A protease affects nuclear localization of 3CD during infection. J. Virol. 90 (24), 11032–11042.
Wang, T., Yu, B., Lin, L., Zhai, X., Han, Y., Qin, Y., Guo, Z., Wu, S., Zhong, X., Wang, Y., Tong, L., Zhang, F., Si, X., Zhao, W., Zhong, Z., 2012. A functional nuclear localization sequence in the VP1 capsid protein of coxsackievirus B3. Virology 433 (2), 513–521.
Waggoner, S., Sarnow, P., 1998. Viral ribonucleoprotein complex formation and nucleolar-cytoplasmic relocalization of nucleolin in poliovirus infected cells. J. Virol. 72, 6699–6709.
Weidman, M.K., Sharma, R., Raychaudhuri, S., Kundu, P., Tsai, W., Dasgupta, A., 2003. The interaction of cytoplasmic RNA viruses with the nucleus. Virus Res. 95 (1-2), 75–85.
Wychowski, C., van der Werf, S., Girard, M., 1985. Nuclear localization of poliovirus capsid polypeptide VP1 expressed as a fusion protein with SV40-VP1. Gene 37 (1–3), 63–71.
Xiang, Q.W., Zou, J.F., Wang, X., Sun, Y.N., Gao, J.M., Xie, Z.J., Wang, Y., Zhu, Y.L., Jiang, S.J., 2013. Identification of two functional nuclear localization signals in the capsid protein of duck circovirus. Virology 436 (1), 112–117.
Xu, Q., Zhang, R., Chen, L., Yang, L., Li, J., Dou, P., Wang, H., Xie, Z., Wang, Y., Jiang, S., 2012. Complete genome sequence of a duck hepatitis a virus type 3 identified in eastern China. J. Virol. 86 (24), 13848.
Zhang, Y., Cao, Q., Wang, M., Jia, R., Chen, S., Zhu, D., Liu, M., Sun, K., Yang, Q., Wu, Y., Zhao, X., Chen, X., Cheng, A., 2017. The 3D protein of duck hepatitis A virus type 1 binds to a viral genomic 3' UTR and shows RNA-dependent RNA polymerase activity. Virus Genes 53 (6), 831–839.
Zhang, Z., Chen, J., Shi, H., Chen, X., Shi, D., Feng, L., Yang, B., 2012. Identification of a conserved linear B-cell epitope in the M protein of porcine epidemic diarrhea virus. Virol. J. 9, 225.